Large angle proton + ^{208}Pb elastic scattering at 800 MeV

L. Ray and G. W. Hoffmann
Department of Physics, The University of Texas at Austin, Austin, Texas 78712
(Received 2 July 1984)

A variety of nuclear structure and proton-nucleus dynamical effects are shown to significantly influence the behavior of the large angle 800 MeV p + ^{208}Pb elastic angular distribution. While coupled channels effects are found to be important, they are significantly smaller than recently suggested.

Recently Amado and Sparrow (AS) (Ref. 1) stated that the large momentum transfer ($q \lesssim 5.3$ fm^{-1}) 800 MeV proton + ^{208}Pb elastic differential cross section data[2] can be reasonably explained by accounting for multistep processes which proceed through the strong, low-lying nuclear collective states, such as the 2.61 MeV 3^-. Previous theoretical calculations which used nonrelativistic optical models or multiple scattering approaches[2,3] did not account for the details of the large angle data. The AS calculations consisted of approximate solutions of the eikonal equations[4] for the proton-nucleus (pA) scattering amplitude. Simple optical potential geometries were used, and spin dependence was neglected.

In this paper we make the following observations: (1) accurate numerical evaluation of the coupled-channels Schrödinger equations with phenomenological optical potentials yields multistep contributions which are similar in trend but considerably smaller in magnitude than the results shown in Fig. 1 of Ref. 1; (2) improved descriptions of the large angle data relative to those obtained from nonrelativistic, spin-dependent, Woods-Saxon optical models are obtained when more realistic densities and effective interaction forms are employed and also when relativistic effects are included; and (3) other contributions, such as correlations and off-shell behavior, are also significant at large momentum transfer. A proper description of high momentum transfer data will therefore demand an exhaustive treatment of many important effects.

To begin with let us consider the influence of intermediate scattering states involving the strong, low-lying collective levels of the target nucleus. Within the context of nonrelativistic multiple scattering theory it is well known that the contributions of intermediate nuclear excitations to proton-nucleus elastic scattering are formally included in the definitions of the optical potentials given by Kerman, McManus, and Thaler (KMT) (Ref. 5) or Watson.[6] For instance, in the Watson approach, the pA elastic scattering t matrix is obtained from the integral equation

$$PTP \equiv T_{00} = U_{\rm opt} + U_{\rm opt} G P T_{00} \ , \tag{1}$$

where

$$U_{\rm opt} = AP\tau P + A(A-1)P\tau GQ\tau P + \cdots \ , \tag{2}$$

$$\tau = v + vGQ\tau \ , \tag{3}$$

and $G = (E - h_0 - H_A + i\epsilon)^{-1}$. In these equations it is assumed that all projectile-target nucleon interactions v are the same; E is the pA energy; h_0 is the pA kinetic energy operator; H_A is the nuclear Hamiltonian; P is the elastic channel projection operator, given by $|\Phi_{\rm g.s.}\rangle\langle\Phi_{\rm g.s.}|$, where $|\Phi_{\rm g.s.}\rangle$ denotes the antisymmetric nuclear ground state; and $Q = \mathring{A} - P$ and $\mathring{A} = \sum |\Phi_i\rangle\langle\Phi_i|$, where the $|\Phi_i\rangle$ represent all antisymmetric (physical) target nucleus states. Intermediate nuclear excitations appear in both the effective interaction operator τ, and in the second and higher order terms of the optical potential.

In actual calculations τ is replaced by either the free proton-nucleon (pN) t matrix[5] or by a density dependent effective interaction which includes effects due to Pauli blocking in an infinite nuclear medium.[7] This procedure thus replaces the nuclear spectrum $|\Phi_i\rangle$ with that of the free two-body system or with a single particle infinite nuclear matter spectrum. The second order correlation terms as included in numerical calculations mainly account for target particle identity, short-range nuclear repulsion, center-of-mass constraints, and intrinsic deformation effects.[8–12] Thus an explicit accounting of strong vibrational nuclear collectivity has been omitted in most multiple scattering calculations. One exception is the work of Chaumeaux, Layly, and Schaeffer,[9] in which long range correlation terms are considered in order to account for nuclear vibrational collectivity. In their work, and in other second order multiple scattering calculations, a number of simplifying assumptions are made for numerical convenience which invalidate the calculation of correlation effects at high momentum transfer. Thus, to account for nuclear collectivity, it is best to retain the original coupled-channels structure of the pA Hamiltonian and absorb only the noncollective channels into the definition of the optical potential.

Reexpressing the target nucleus projection operator $\mathring{A}$ as $(P + Q_c + Q')$, where

$$Q_c = \sum_{i=\text{collective}} |\Phi_i\rangle\langle\Phi_i| \ ,$$

projects out the dominant collective vibrational states, and $Q' = Q - Q_c$, the pA scattering operator with explicit channel coupling, can be expressed as

$$T=\tilde{U}+\tilde{U}G(P+Q_c)T\ , \tag{4}$$

$$\tilde{U}=A\tilde{\tau}+A(A-1)\tilde{\tau}GQ'\tilde{\tau}+\cdots\ , \tag{5}$$

and

$$\tilde{\tau}=v+vGQ'\tilde{\tau}\ , \tag{6}$$

where $\tilde{U}$ and $\tilde{\tau}$ represent the optical potential and effective interaction in the explicit coupled-channels representation. The coupled operator equations for pA elastic and collective inelastic channels, corresponding to Eq. (4), are given by

$$T_{00}=\tilde{U}_{00}+\tilde{U}_{00}GPT_{00}+\tilde{U}_{0c}GQ_cT_{c0}\ , \tag{7a}$$

$$T_{c0}=\tilde{U}_{c0}+\tilde{U}_{c0}GPT_{00}+\tilde{U}_{cc}GQ_cT_{c0}\ , \tag{7b}$$

where $T_{00}\equiv PTP$, $T_{c0}\equiv Q_cTP$, $\tilde{U}_{00}\equiv P\tilde{U}P$, $\tilde{U}_{c0}\equiv Q_c\tilde{U}P$, etc.

It should be emphasized that the pA elastic scattering t matrix in Eq. (7) is equivalent to that in Eq. (1). Differences arise, however, when numerical approximations are made. As already discussed, in practical calculations explicit treatment of nuclear collectivity is lost when evaluating T_{00} via Eqs. (1)–(3); it can be retained by way of Eqs. (5)–(7). Notice that the elastic channel diagonal projection of $\tilde{U}$ differs from $U_{\rm opt}$ of Eq. (2) by the omission of the intermediate nuclear collective channels which are explicitly contained in the coupled equations. Thus in a rigorous microscopic calculation which includes explicit channel coupling, the elastic channel optical potential is $\tilde{U}_{00}$, not $U_{\rm opt}$. In the present work such differences will be absorbed in the optical model phenomenology.

To investigate the effect of explicit channel coupling to nuclear vibrational collective states, several calculations were performed in which *phenomenological* models for $\tilde{U}$ were assumed. To begin we used a standard twelve-parameter Woods-Saxon optical potential model to fit the forward angle ($\leq 22°$ c.m.) p+^{208}Pb angular distribution data; the following optical potential parameters were obtained:[13] V, W, $V_{\rm SO}$, $W_{\rm SO}$, r, a, r_w, a_w, $r_{\rm SO}$, and $a_{\rm SO}$ are −4.63, 53.9, 0.51, and 0.95 MeV, and 1.075, 0.753, 1.123, 0.615, 1.111, and 0.671 fm, respectively. The fit (solid curve in Fig. 1) to the forward angle data (as well as the elastic analyzing power data[3]) is good. Next, a coupled-channels calculation was done in which the 0^+ ground state, and the 2.61 MeV 3^- and 4.1 MeV 2^+ states were coupled using the Woods-Saxon optical potential for the diagonal terms and derivative forms for the coupling potentials.[14] Channel coupling via the spin-orbit force was omitted. The coupling strengths for the 3^- and 2^+ excitations were artificially increased to mock up further collective state coupling as in Ref. 1. Based on the analysis of Gazzaly *et al.*[15] of 800 MeV p+^{208}Pb collective excitations we set

$$\sum_{J^\pi=3^-,2^+}|\delta_{J^\pi}|^2/|\delta^*_{3^-}|^2=2.7\ ,$$

and let $\delta_{3^-}=\delta_{2^+}$; the macroscopic deformation lengths, δ_{J^π}, are defined in Refs. 1 and 15. The 2.61 MeV 3^- deformation length obtained in Ref. 15 is denoted by $\delta^*_{3^-}$. The calculations were performed using the coupled channels code JUPITER,[16] modified to include relativistic kinematics and an extended number of partial waves and mesh points needed for accuracy. The elastic channel diagonal potential assumed is the same as already given, except that (r_w,a_w) were slightly adjusted to (1.136,0.598) fm in order to recover the fit to the forward angle data.

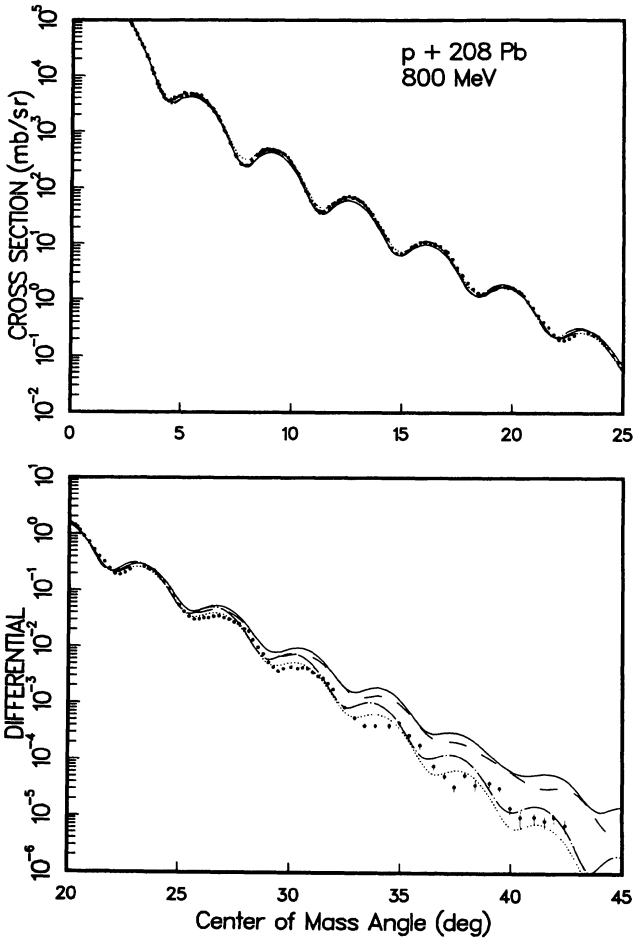

FIG. 1. Angular distributions for 800 MeV p+^{208}Pb elastic scattering. Data are from Ref. 2. The Woods-Saxon optical model result (no coupling) is indicated by the solid curve, the coupled channels calculation by the dashed line, the KMT result (no coupling) by the dash-dot curve, and the RIA result by the dotted line. In all cases the fits to the forward angle data were $|\chi|^2$ optimized.

The results, indicated by the dashed curve in Fig. 1, demonstrate that the net effect, at large angles, of explicit coupling to nuclear collective levels is to reduce in magnitude and shift to slightly larger angles the maxima and minima of the predicted differential cross section. As found by AS, the coupled channels effects begin to be apparent at angles for which the elastic and collective inelastic cross sections are comparable in magnitude. The separate effects of coupling to the 2^+ and 3^- are merely additive in their impact on the large angle elastic cross

section so that constructive rather than destructive interference between the two multistep processes occurs. Furthermore, very little j-transfer dependence is noted in the multistep contributions to the elastic channel.

Although the trends of these channel coupling effects are in agreement with AS, important differences exist. For example, the calculations reported here indicate cross section reductions varying from 10% at 27° to 30% at 37°, whereas AS report reductions varying from 50% to 80% at these same angles. We therefore disagree with AS, who find that coupling to nuclear collective states is almost sufficient to resolve the discrepancies between simple optical model calculations and the large angle data.

First order microscopic optical model calculations were also done using the KMT potential[8] generated from realistic densities and pN effective interactions, but with no explicit channel coupling. The first order, spin dependent KMT optical potential (see Ref. 8) was obtained using the proton densities determined from analysis of electron scattering measurements,[17] the ^{208}Pb neutron density predicted by Dechargé and Gogny,[18] and the pN scattering amplitudes of Arndt *et al.*[19] The optimally factorized local optical potential prescription of Ref. 20 utilizing Breit frame kinematics was employed. Nucleon-nucleon (NN) phase shifts from 800 to 1000 MeV were used in calculating the optical potential form factor out to the large momentum transfers required (6 fm^{-1}). The forward angle data were fit by adjusting the surface geometry of the neutron density. The assumed neutron distribution was taken as

$$\rho_n(r)=\rho_{n,\text{theo}}(r)+\text{WS}(r)-\text{WS}_{\text{STD}}(r)\ , \tag{8}$$

where $\rho_{n,\text{theo}}(r)$ is the theoretical neutron density distribution of Dechargé and Gogny,[18] WS(r) is a Woods-Saxon function normalized to 126 neutrons whose radius and diffuseness were varied in the fitting process, and $\text{WS}_{\text{STD}}(r)$ is a fixed Woods-Saxon form also normalized to 126 neutrons with radius and diffuseness chosen to reproduce the surface region of $\rho_{n,\text{theo}}(r)$. The resulting fit to the forward angle data and subsequent large angle predictions are shown by the dash-dot curve in Fig. 1. Considerable improvement over the Woods-Saxon optical model result is obtained simply by using more realistic optical potential geometries.

Next, a relativistic impulse approximation (RIA)-Dirac equation calculation[20,21] was done. No explicit channel coupling was included. The proton and neutron vector densities[21] were set equal to those used in the nonrelativistic KMT calculation. The scalar densities were obtained from the Dirac-Hartree model of Serot[22] according to the prescription[21]

$$\rho^{p,n}_{\text{scalar}}(r)=\rho^{p,n}_{\text{vector}}(r)+[\rho^{p,n}_{\text{scalar}}(r)-\rho^{p,n}_{\text{vector}}(r)]_{\text{Serot}}\ , \tag{9}$$

where the densities in the square brackets are the theoretical Dirac-Hartree densities.[22] The relativistic invariant pN amplitudes were obtained as discussed in Refs. 20 and 21 to 6 fm^{-1} using the same Arndt phase shifts that were used for the KMT calculation. Solution of the Dirac equation with complex scalar and timelike vector component optical potentials (tensor contributions are negligible; see Ref. 23) yields the elastic scattering observables; the differential cross section is shown in Fig. 1 by the dotted curve. The neutron vector density was varied according to Eq. (8) to fit the forward angle ($\leq 25°$ c.m.) differential cross section data. The neutron scalar density was recomputed at each step of the search procedure according to Eq. (9).

The principal differences in physical content between the relativistic and nonrelativistic calculations are (1) inclusion of intermediate negative energy states of the projectile (i.e., virtual pair processes), and (2) relativistic nuclear structure effects (i.e., lower components for target wave functions) represented by the scalar-vector density difference.[22] A relativistic impulse calculation was also made with

$$\rho_{\text{scalar}}(r)=\rho_{\text{vector}}(r)\ ,$$

separately for protons and neutrons, in which the forward angle data were fit by varying the neutron vector density as in Eq. (8). From this it is observed that including the virtual pair processes brings about the shift (compared to the KMT result) in the angular distribution to larger angles, while permitting lower components in the target wave functions suppresses the magnitude of the back angle cross section prediction.

Many other effects are likely to be important at high momentum transfer, but as yet, reliable calculations remain to be made. The effects of fully folding the first order optical potential and off-shell NN t-matrix contributions have been considered for pA scattering at lower energies.[24] Calculations indicate that these effects might be fairly large at high momentum transfer.[24] Medium effects in the pN effective interaction have only been realistically calculated at energies below pion production threshold.[7] Preliminary results[25] indicate a diminution in Pauli blocking effects above 500 MeV, but complete calculations remain to be made. Nonrelativistic second order optical potential contributions (i.e., those due to correlations) have been estimated,[8–12] but none of these are reliable at large momentum transfer. Most calculations that include correlations show an enhancement of the large angle differential cross sections. This can be seen by comparing the first order KMT (dash-dot curve) result in Fig. 1 with the second order KMT calculation shown in Fig. 5 of Ref. 3. Correlation effects computed by Varma and co-workers[12] for this case indicate both an enhancement and angle shift.

In conclusion, it has been shown that coupled channels effects for 800 MeV p+^{208}Pb, due to intermediate excitation and deexcitation of strong nuclear collective states (via phenomenological Woods-Saxon potentials), become noticeable at angles where the magnitudes of the elastic and inelastic cross sections are comparable, in agreement with AS. The effect on the elastic differential cross section at high momentum transfer is to reduce in magnitude and shift to larger angles the angular distribution, although by an amount much less than reported by AS. More realistic optical potentials (of the KMT variety) and relativistic effects (RIA-Dirac calculations) also produce considerable improvement in the description of the large angle data compared to that of nonrelativistic Woods-

Saxon optical models. Coupled-channels relativistic calculations have not been carried out, but will be considered in future analyses of these data. The results in Fig. 1 suggest that such calculations might be quite successful. We caution, however, that other theoretical corrections (e.g., correlations, full folding, off-shell dependences, medium modifications, etc.) will undoubtedly play a significant role at the large momentum transfers under consideration, so that a satisfactory theoretical understanding of large angle pA phenomena must await further theoretical and numerical work.

This research was supported in part by The Robert A. Welch Foundation and the U. S. Department of Energy.

[1]R. D. Amado and D. A. Sparrow, Phys. Rev. C **29**, 932 (1984).
[2]G. W. Hoffmann *et al.*, Phys. Rev. C **21**, 1488 (1980).
[3]G. W. Hoffmann *et al.*, Phys. Rev. C **24**, 541 (1981).
[4]R. J. Glauber, in *Lectures in Theoretical Physics*, edited by W. E. Brittin and L. G. Dunham (Interscience, New York, 1959), p. 315.
[5]A. K. Kerman, H. McManus, and R. M. Thaler, Ann. Phys. (N.Y.) **8**, 551 (1959).
[6]K. M. Watson, Phys. Rev. **89**, 575 (1953).
[7]J. P. Jeukenne, A. Lejeune, and C. Mahaux, Phys. Rev. C **10**, 1391 (1974); H. V. von Geramb, in *The Interaction Between Medium Energy Nucleons in Nuclei—1982* (Indiana University Cyclotron Facility), Proceedings of the Workshop on the Interaction Between Medium Energy Nucleons in Nuclei, AIP Conf. Proc. No. 97, edited by H. O. Meyer (A.I.P., New York, 1983), p. 44.
[8]L. Ray, Phys. Rev. C **19**, 1855 (1979); L. Ray, G. W. Hoffmann, and R. M. Thaler, *ibid.* **22**, 1454 (1980); L. Ray and M. M. Gazzaly, Phys. Lett. **124B**, 309 (1983).
[9]A. Chaumeaux, V. Layly, and R. Schaeffer, Ann. Phys. (N.Y.) **116**, 247 (1978).
[10]H. Feshbach, A. Gal, and J. Hüfner, Ann. Phys. (N.Y.) **66**, 20 (1971).
[11]P. Osland and R. J. Glauber, Nucl. Phys. **A326**, 255 (1979).
[12]D. R. Harrington and G. K. Varma, Nucl. Phys. **A306**, 477 (1978); G. K. Varma and L. Zamick, *ibid.* **A306**, 343 (1978).
[13]The optical potential parameter notation is that of C. M. Perey and F. G. Perey, At. Data Nucl. Data Tables **13**, 293 (1974).
[14]T. Tamura, Rev. Mod. Phys. **37**, 679 (1965).
[15]M. M. Gazzaly *et al.*, Phys. Rev. C **25**, 408 (1982).
[16]T. Tamura, Oak Ridge National Laboratory Report No. ORNL-4152, 1967 (unpublished).
[17]B. Frois *et al.*, Phys. Rev. Lett. **38**, 152 (1977).
[18]J. Dechargé and D. Gogny, Phys. Rev. C **21**, 1568 (1980); J. Dechargé, private communication.
[19]R. A. Arndt *et al.*, Phys. Rev. D **28**, 97 (1983). The SP82 solution was used.
[20]J. A. McNeil, L. Ray, and S. J. Wallace, Phys. Rev. C **27**, 2123 (1983).
[21]J. A. McNeil, J. Shepard, and S. J. Wallace, Phys. Rev. Lett. **50**, 1439 (1983); J. Shepard, J. A. McNeil, and S. J. Wallace, *ibid.* **50**, 1443 (1983); B. C. Clark, S. Hama, R. L. Mercer, L. Ray, and B. D. Serot, *ibid.* **50**, 1644 (1983); B. C. Clark, S. Hama, R. L. Mercer, L. Ray, G. W. Hoffmann, and B. D. Serot, Phys. Rev. C **28**, 1421 (1983).
[22]C. J. Horowitz and B. D. Serot, Nucl. Phys. **A368**, 503 (1981); B. D. Serot, private communication.
[23]B. C. Clark *et al.*, Phys. Rev. Lett. **51**, 1808 (1983).
[24]A. Picklesimer, P. C. Tandy, R. M. Thaler, and D. H. Wolfe, Phys. Rev. C **29**, 1582 (1984).
[25]L. Ray (unpublished).